Q2D-morfo: a medium to long term model for beach morphodynamics

A. Falqués & R. Garnier
Technical University of Catalonia, Barcelona, Catalonia, Spain
E. Ojeda, F. Ribas, & J. Guillen
Institute of Marine Sciences, CSIC, Barcelona, Catalonia, Spain

ABSTRACT: An extension of one-line coastline models to include cross-shore beach profile dynamics is presented. The extension is in the same direction as the existing N-line models but the rationale is different. The new model updates the bed levels by considering sediment conservation in two horizontal dimensions rather than moving the contour lines or layers. In this sense it is like a 2DH model but is not fully 2DH because sediment transport is directly parameterized from the wave field without solving for the mean hydrodynamics. The model is tested against la Barceloneta beach (Barcelona) evolution during a 35-day period including two storms. Preliminary results indicate that even though the model largely overpredicts the shoreline retreat, the overall qualitative erosion/accretion tendencies are well reproduced.

1 INTRODUCTION

In spite of the complexity of 3D nearshore morphodynamics, the so-called one-line modelling has had some success in understanding and predicting the dynamics of sandy coastlines at large space and time scales (Pelnard-Considère 1956; Larson et al. 1987; Larson and Kraus 1991; Komar 1998). This is a severe simplification and consists in averaging on the vertical and the cross-shore directions so that the morphodynamical active region collapses in a single line which represents the coastline. The changes in coastline position are then given by convergence/divergence of the total alongshore sediment transport rate Q which is determined just by the wave forcing without account of surf zone hydrodynamics (water inertia, mass conservation, etc.). Cross-shore sediment transport is not explicitly considered although it is always implicit to ensure the sediment redistribution that is necessary to reach the equilibrium beach profile after the changes which are driven by alongshore transport.

The standard one-line modelling has however a number of important shortcomings. First, a stable shoreline is always predicted in contrast with the finding of Ashton et al. (2001) (see also, Falqués and Calvete (2005) and Ashton and Murray (2006)) according to which the shoreline may become unstable if the wave incidence angle is large enough. Even in case where the coastline is stable, the standard one-line modelling over-predicts the shoreline diffusivity (Falqués 2003). Second, the governing equation for small deviations from a rectilinear shoreline is a diffusion equation. This precludes the modelling of shoreline sand wave propagation which are sometimes observed (Inman 1987; Thevenot and Kraus 1995; Ruessink and Jeuken 2002; Falqués and Calvete. 2003; Falqués 2006). These two drawbacks are caused by the fact that the traditional one line modelling neglects the effect of nearshore bathymetric changes associated to changes in coastline on the wave transformation (Falqués and Calvete 2005).

Falqués and Calvete (2005) have developed a linear stability model of the coastline based on the one-line concept but including the bathymetric changes associated to coastline changes in a simplified way. This model describes shoreline instability and sand wave propagation. It has nevertheless a number of limitations. First, the cross-shore profile dynamics which is proven to be crucial for that instability (Falqués and Calvete 2005) is ignored and a fixed cross-shore shape function is considered for the bathymetric signal of the shoreline disturbances. Second, as it is a linear stability model it only allows for small amplitude departures of a rectilinear coastline. Since it is based on an analysis of alongshore propagating harmonic modes on an open coast it is not straightforward how to adapt it to bounded beaches. Similarly, the model is aimed at the free dynamic problem of the coastline and, again, the adaptation to a forced problem (e.g. propagation of sand waves along a sandy coast under the forcing by an adjacent tidal inlet dynamics,

see (Falqués 2006)) is not obvious. Finally, the wave driver is fixed, simply consisting of the wavenumber irrotationality, wave energy conservation and dispersion relation.

The aim of the present contribution is setting up an extension of one-line shoreline models with the following characteristics: i) including the cross-shore sediment transport in a parametric way, ii) keeping the capabilities of the linear stability model of Falqués and Calvete (2005) and iii) performing non-linear time evolution (arbitrary geometry, no small amplitude restriction). The sediment transport is considered in two dimensions on the whole nearshore, not only at the coastline as the one-line models. Also, the wave propagation on the evolving 2DH topography is considered. By these two reasons it is a 2DH model. However, the nearshore hydrodynamics is not considered because the sediment transport is computed directly from the wave field through parameterizations as the CERC formula for the littoral drift. This assumption filters out all the rich self-organized morphodynamic processes of the surf zone associated to rip currents and meandering longshore current (see, for instance, Calvete et al. (2005) and Garnier et al. (2006)). This is the most important limitation of the model and poses an evident lower bound to the resolved lengthscales which is in the order of the surf zone width. In this sense the new model is only quasi-2DH. In other words, it is equivalent to the N-line shoreline models (Steetzel et al. 1998; Dabees and Kamphuis 2000).

Along with the model setup we here present a test of the model against the changes of La Barceloneta beach, in Barcelona, during October-November 2003.

2 THE MODEL

2.1 Geometry, integration domain and grid

The integration domain is inside the rectangular and horizontal domain $\{0 \leq x \leq L_x; 0 \leq y \leq L_y\}$. The y axis is chosen with an orientation similar to the mean orientation of the initial shoreline and in such a way that there is some distance between the axis and the initial shoreline. A rectangular grid is chosen, running from $i = 0$ up to $i = n$ in the direction of the x axis and from $j = 0$ up to $j = m$ in the direction of the y axis. A staggered grid is also defined, from $ic = 1$ up to $ic = n$ and from $jc = 1$ up to $jc = m$. If the grid spacings are $\Delta x = L_x/n, \Delta y = L_y/m$, the basic grid is defined as:

$$x(i) = i\,\Delta x \quad i = 0, 1, 2, ...n$$

$$y(j) = j\,\Delta y \quad j = 0, 1, 2, ...m \tag{1}$$

and the staggered one is defined as:

$$x(ic) = x(i) - \Delta x/2 \quad i = ic, \quad ic = 1...n$$

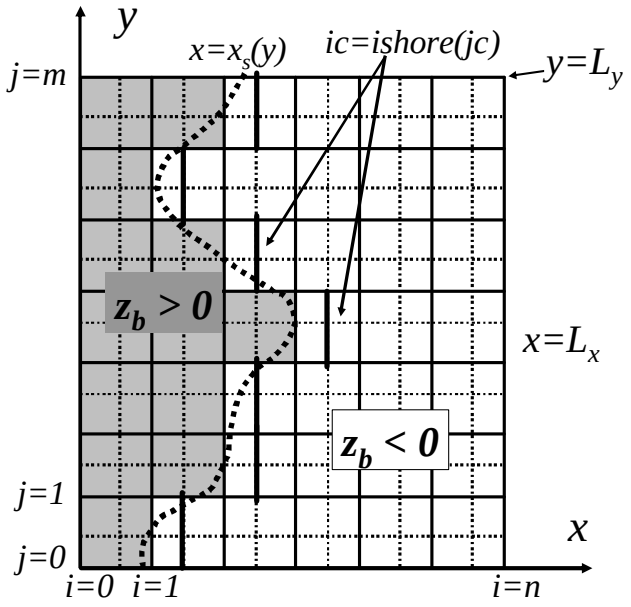

Figure 1. Geometry of the domain and integration grid.

$$y(jc) = y(j) - \Delta y/2 \quad j = jc, \quad jc = 1...m \tag{2}$$

The topography is given by $z = z_b(x, y)$ and $z = z_s$ defines the mean water level. The grid position of the shoreline is defined by $ic = ishore(jc)$ which is the smallest ic such that $D(x(ic), y(jc)) = z_s - z_b(x(ic), y(jc)) \geq 0$. By linear interpolation between $z_b(x(ic), y(jc))$ and $z_b(x(ic-1), y(jc))$ the cross-shore position $x_s(y)$ where $D(x_s(y), y) = 0$ is computed. The $x = x_s(y)$ line determines a smooth shoreline. For certain applications, the wave set-up can be incorporated. This may be done by computing the total approximated set-up at the shoreline $z_{su} = 0.15H_b$ (Short 1999).

2.2 Dynamical equation: sediment conservation

The dynamical equation in the model is the sediment conservation in two horizontal dimensions

$$\frac{\partial z_b}{\partial t} + \frac{\partial q_x}{\partial x} + \frac{\partial q_y}{\partial y} = 0 \tag{3}$$

where $\vec{q}$ is the horizontal depth-integrated sediment flux ($m^3/m/s$) along with the shoreline updating algorithm which is described in Sec. 2.5. The porosity factor is included in the expression of $\vec{q}$ as $1/(1-p)$. This equation is discretized on all the wet cells, $ic \geq ishore(jc)$, by using an explicit second order Adam-Bashforth scheme in time (Garnier et al. 2006) and finite differences in space:

$$zb^k_{ic,jc} = zb^{k-1}_{ic,jc} - (\frac{3}{2}\,div^{k-1}_{ic,jc} - \frac{1}{2}\,div^{k-2}_{ic,jc})\,\Delta t \tag{4}$$

with

$$1 \leq jc \leq m\,, \quad ishore(jc) \leq ic \leq n\,, \quad k \geq 2$$

and

$$div^k_{ic,jc} = \frac{q_x(i,jc)^k - q_x(i-1,jc)^k}{\Delta x} + \frac{q_y(ic,j)^k - q_y(ic,j-1)^k}{\Delta y}$$

with

$$1 \leq jc \leq m\,, \quad ishore(j) \leq ic \leq n\,,$$

$$i = ic\,, \quad j = jc\,, \quad k \geq 0$$

The sediment flux, $\vec{q}$, can be parameterized with a number of different formulations and this is described in Sec. 2.4.

2.3 Wave driver

To compute the sediment flux, the wave height H_b and direction θ_b at breaking are needed while wave characteristics are given at the offshore boundary of the domain, $x = L_x$. Thus, the wave transformation from the offshore boundary up to breaking must be determined. This can be done in different ways, but the external RefDif model which solves a parabolic approximation of the mild slope equation (Kirby and Dalrymple 1994) has been used for the application shown here.

2.4 Sediment transport

The crucial simplification in the model which makes it different from fully 2DH models is the computation of sediment transport. In fully 2DH models, the mean horizontal hydrodynamics is computed from the incident wave field and the sediment transport is then evaluated. Here, the sediment transport is directly computed from the wave field by using parameterizations. This is in line with one-line and N-line models. It implies a very drastic simplification since the hydrodynamics (longshore current, sea surface setup/setdown, rip currents, ...) does not need to be computed. This is however the main limitation of the model.

In view of the previous experience regarding one-line and N-line models, the sediment flux in the model reads as

$$\vec{q} = \vec{q}_L + \vec{q}_C \tag{5}$$

The first term represents the alongshore wave-driven transport (or littoral drift) which is due to the longshore current driven by the breaking waves in case of off-normal wave incidence. It is evaluated here by first computing the total sediment transport rate, i.e., cross-shore integrated flux with the so-called generalized CERC formula (Komar 1998; Horikawa 1988):

$$Q = \mu H_b^{5/2} \left(\sin(2\alpha_b) - \frac{2r}{\beta} \cos(\alpha_b) \frac{\partial H_b}{\partial y'} \right) \tag{6}$$

where $H_b(y)$ is the (rms) wave height and $\alpha_b = \theta_b(y) - \phi(y)$ is the angle between wave fronts at breaking and coastline. The constant in front of it is of order $\mu \sim 0.1 - 0.2$ m$^{1/2}$s^{-1} and β is the beach slope at the shoreline. The value $r = 1$ has been used. Then, the sediment flux is computed by multiplying the total transport rate by a function $f(x)$ which represents the cross-shore distribution of Q:

$$\vec{q}_L = f(x)Q(y)(\sin\phi(y), \cos\phi(y)) \tag{7}$$

and by considering the deviation of the local orientation of the coastline with respect yo the y axis, $\phi(y)$. Actually, the $\phi(y)$ angle is computed not as the angle between the shoreline itself and the y axis, but as the mean orientation of the bathymetric lines in the surf zone and the y axis. This is the 'mean' shoreline orientation felt by the waves.

The second term in 5, $\vec{q}_C$, accounts for all the contributions in sediment transport not included in the first term. Although it is commonly weaker, its evaluation is by far much more complex. This is the sediment flux which is believed to build up the equilibrium beach cross-shore profile in case of shore-normal wave incidence. It primarily consists of the down-slope transport due to gravity, the onshore transport due to wave nonlinearities and the offshore transport due to undertow. This part of the model is still under development since many possible options are to be explored. Up to now, two main options have been explored: i) relaxation to a given equilibrium beach profile and ii) the use of the Bailard formulation (Bailard 1981).

For the first option, some equilibrium profile $z_b = h(x)$ is assumed depending on sediment size and incident wave energy so as the equilibrium bathymetry is $z_b = z_{be}(x,y) = h(x - x_s(y))$. Alternatively, in modelling a particular beach, the equilibrium profile can be defined from the observations at this particular beach. The sediment flux is computed in this option as:

$$\{\vec{q}_C\}_x = -\gamma_x \left(\frac{\partial(z_b - z_{be})}{\partial x}\right), \quad \{\vec{q}_C\}_y = -\gamma_y \frac{\partial z_b}{\partial y} \tag{8}$$

By inserting this expression into eq. 3 it is immediately seen that γ_x, γ_y play the role of cross-shore and longshore diffusivities. Again there are many options to describe such diffusivities which are the result of many complex and unknown processes. The

alongshore diffusivity is primarily caused by downslope gravitational transport and the cross-shore diffusivity is caused by the combination of that transport with undertow and wave nonlinearities. On the other hand, the overall philosophy of the model and the corresponding parameterizations do not make sense at scales smaller that the surf zone width. In contrast, the numerics of the model drives the topographic evolution at the grid spacing scale ($\Delta x, \Delta y$) and this may cause the growth of small scale instabilities that can not be controlled by the large scale physics described by the model. To keep control of those processes at the grid spacing scale there is the need for a background diffusivity. Thus, rather than evaluating the diffusivity from the detailed description of downslope transport and other processes, we follow a heuristic approach and we assume for the time being that these diffusivity coefficients are proportional to the momentum diffusivity in the surf zone coming from the turbulence generated by wave breaking, $\nu_t = M(\mathcal{D}/\rho)^{1/3}H$, where M is a constant, ρ is water density, H is rms wave height and $\mathcal{D}$ is wave energy dissipation. Thus, $\gamma_x(x), \gamma_y(x)$ are assumed to be proportional to the mean ν_t in the surf zone, multiplied for a shape function of x that makes it maximum at the surf zone and makes it to decay beyond the breaker line and with nondimensional factors, $\epsilon_{xm}, \epsilon_{ym}$.

In the second option, some parameterizations of the wave nonlinearities and undertow are used to feed in the Bailard formula (Bailard 1981). The downslope transport could also been computed by that formula, but this gives unrealistically small bed-slope coefficients (γ_x, γ_y) so that the expressions based on ν_t where also used in this formulation. Much work has been devoted to test model behaviour with this option. In many cases the beach tends to certain sensible equilibrium bathymetry but in some cases numerical instabilities arise and the model crashes. This is currently under investigation. By this reason, we have selected the first option for the present application to La Barceloneta beach. As equilibrium beach profile, the alongshore average of the bathymetry observed on October 1, 2003, has been used for the runs presented here.

2.5 Coastline evolution

At each time step, $t = k\Delta t$, and starting from the previous bathymetry, $zb^{k-1}_{ic,jc}$, the discretized sediment conservation eq. 4 is applied to all cells including those next to the shoreline to obtain a first approximation to the updated bathymetry, $[zb^k_{ic,jc}]_0$. The resulting new position of the shoreline, $i = [ishore(j)^k]_0$, is then found. After this, the bed level of the cells neighboring the shoreline is changed in order to have a prescribed slope $\beta(y)$ at the shoreline and to conserve sediment. This modification is done by rotating the bed surface around a horizontal axis which is tangent to the local shoreline at each $y(jc)$. This may change the bed level at those cells giving rise to a new bathymetry, $[zb^k_{ic,jc})]_1$. The resulting new position of the shoreline, $i = [ishore(j)^k]_1$, is again determined. The procedure is repeated until no change is detected so as the true bathymetry , $zb^k_{ic,jc}$ and shoreline position, $i = ishore(j)^k$, are obtained. Usually, only one iteration is needed for each time step.

The prescribed slope of the swash zone may be computed with the empirical expression of Sunamura (Short 1999)

$$\beta = 0.12 g D_s \left(\frac{T}{H_b}\right)^2 \tag{9}$$

where D_s is the sediment grain diameter, H_b is the wave height at breaking and T is the wave period.

2.6 Boundary conditions

The governing equation, eq. 3, together with shoreline evolution determine a non-local dynamical system. However, disregarding shoreline changes and the terms arising from $\vec{q}_L$, a second order parabolic equation results from where Dirichlet, Newman or mixed boundary conditions seem appropriate. Thus we have applied

$$\{\vec{q}_C\}_x = 0 \tag{10}$$

at the shoreline which is equivalent to the Newman condition, $\gamma_x \partial(z_b - h(x))/\partial x = 0$. Notice that this does not imply that there is no sediment transport at the shoreline, since the readjustment of bed level at the shoreline cells following the algorithm described in sec. 2.5 to meet the prescribed swash zone slope imply sediment exchange in the cross-shore direction.

At the groins, the condition $\{\vec{q}\}_y = 0$ is considered. At the lateral boundaries offshore of the groins and at the offshore boundary, the relaxation towards some equilibrium is imposed which results in mixed conditions. For instance, at $y = L_y$,

$$\{\vec{q}_C\}_y = \gamma_y \lambda_y^{-1}(z_b - h(x)) \tag{11}$$

is imposed, which is equivalent to

$$\frac{\partial(z_b - h(x))}{\partial y} = -\lambda_y^{-1}(z_b - h(x)) \tag{12}$$

where the relaxation distance is λ_y.

3 THE DATA SET

3.1 La Barceloneta Beach

The Catalan coast is a micro-tidal zone (range $<$ 20 cm) where waves are the main stirring mechanism controlling coastal evolution. The most energetic storms approach from the East with a typical

duration of few days and are typically associated with the cyclonic activity in Western Mediterranean. The annual mean significant wave height (H_s) is lower than 1.0 m but storms can reach maxima H_s near 6 m, with occasionally reaching 10 m. The city of Barcelona is located in the North-western Mediterranean, flanked by two rivers -Besos in the north and Llobregat in the southern part. It has approximately 13 km of coastline containing the city harbour in the southern-most part of the city, three marinas and more than three kilometres of beaches.

La Barceloneta beach is a bar/terraced beach of about 1300 m length which is bounded by the Barcelona Harbour dike to the south and by the Somorrostro dike to the north (see Fig. 3). Its orientation is approximately 20^o. Beach sediment is composed by sands with some proportion of gravels. The median grain size (D_{50}) shows high spatial and temporal variability with an average median grain size of about 1 mm.

3.2 Wave forcing during October-November 2003

We here apply the model to the evolution of La Barceloneta beach during the period from October 1 till November 4, 2003. Deep water wave data are taken from WANA model data set (Puertos del Estado, http://www.puertos.es. See Ojeda and Guillén (2006)) at 63 m water depth. During this period two main storms occurred. The first one was an eastern storm and lasted from 15th to 20th October (see Fig. 2). The peak H_s was 3.4 m, with $T_p = 10.2$ s and direction from 83^o. The second one was a S-SW storm which lasted from October 30 till November 1. The peak H_s was 4.0 m, with $T_p = 9.2$ s and direction from 194^o. The direction of the waves with respect to the shore normal was -26^o in case of the E storm and $+84^o$ for the S-SW. The wave characteristics at the offshore boundary of the model domain (20 m water depth) were $H_s = 3.1$ m, $\theta = -20^o$ during the E storm and $H_s = 1.6$ m, $\theta = 55^o$ during the S-SW one. A striking reduction in wave energy occurred due to wave refraction during the S-SW event.

3.3 Behaviour of the beach

The bathymetry of La Barceloneta beach was measured both on October 1 and on November 3. Figures 3 and 5 show that many complex changes occurred in the bathymery, the most prominent being the following:

1. In water depths between 0 and $3 - 4.5$ m (depending on alongshore location) there was generalized erosion except in the region $350 < y < 600$ m. At some point the bed level decrease reached 1.5 m. (e.g., around $x \simeq 100, y \simeq 700$ with initial bed level, $z_{b0} \simeq = -1.5$ m).

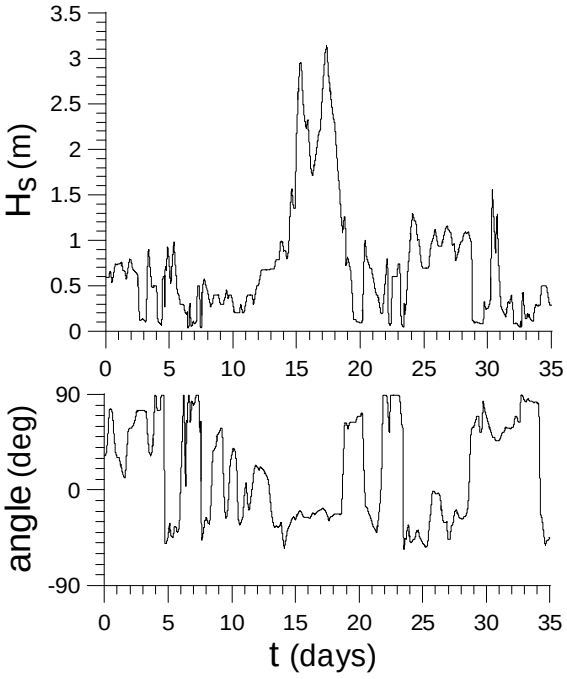

Figure 2. Significant wave height and wave angle at the offshore boundary of the model domain during the simulation period, from October 1 till November 4, 2003. The angles are with respect to shore normal (x-axis), positive from S, negative from E.

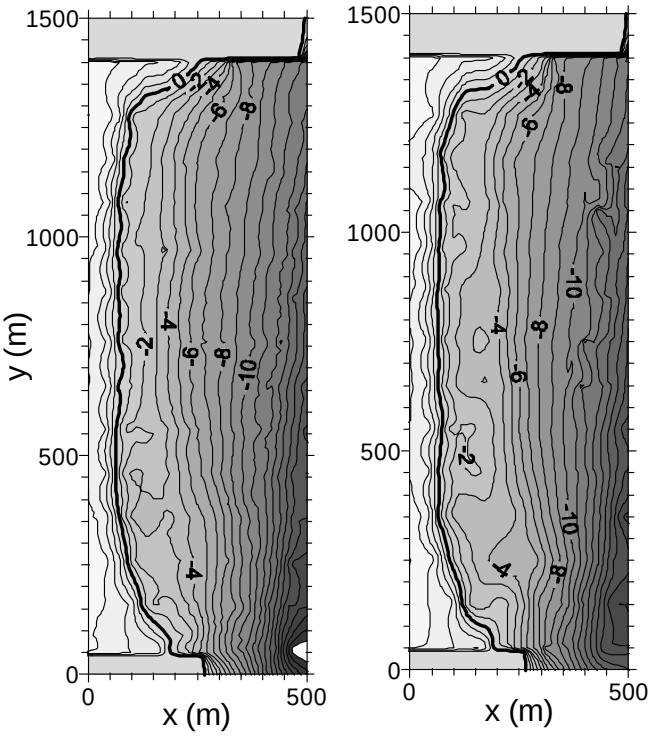

Figure 3. Surveyed bathymetry of La Barceloneta beach. The shoreline is indicated by a thicker line. Left: October 1, 2003. Right: November 3, 2003.

2. In water depths between 3 and 7 m there was mainly deposition except in the region $75 < y < 325$ m. This resulted in a kind of terraced profile (barred at some sections). This deposition area attached to the shore in the region $350 < y < 600$ m. At some places, the bed rose up to 1 m.

3. At the stretch of shore where the deposition attached to the shore, a megacusp developed.

4. Shoreline changes are very minor, not larger than about 15 m.

5. An area of strong deposition appears around $x \simeq 500, y \simeq 50$ m which is very likely an artifact of the gridding due to the proximity of the lowest available bed levels in the bathymetric data.

4 MODEL RUNS

4.1 Parameter setting

The size of the integration domain was $L_x = 1000, L_y = 1500$ m and the grid was chosen as $\Delta x = \Delta y = 10$ m. The model was fed with the initial bathymetry ($t = 0$ at October 1, 0 hr) and was run for 35 days with the observed wave forcing. The morphodynamic time step was $dt = 0.0001$ d and the time step for running RefDif was $dt_w = 0.001$ d (it may seem unnecessarily small, but we observed that larger values might originate numerical instabilities in the morphodynamic model). It turned out that this combination of dt and $\Delta x, \Delta y$ fulfilled the Courant numerical stability condition for the chosen diffusivity coefficients, ϵ_x, ϵ_y, even in the most critical situation which is during the E storm (maximum diffusivity due to maximum energy dissipation). A breaking index $\gamma_b = 0.5$ was assumed, $\mu = 0.15$ m$^{1/2}$s^{-1} and $r = 1$. The relaxation distances for the boundary conditions were set to $\lambda_x = \lambda_y = 2000$ m. The grain size was set to $D_{50} = 0.001$ m.

The most important parameter tuning affecting model outputs is that of the morphodynamic diffusivity coefficients, ϵ_x, ϵ_y. Default values for the present runs were $\epsilon_x = 0.02, \epsilon_y = 0.03$. This means, in dimensional terms, a peak diffusivity of $\gamma_x = 0.038$ m^{2}s^{-1} for the E storm (i.e., $H_s = 3.1$ m, the diffusivity scaling with $H_b^{11/6}$). The criteria used for selecting the sensitivity range are the following. First, there is an upper bound for the morphodynamic diffusivity which is the coastline diffusivity caused by the longshore transport according to the standard one-line modelling, $\gamma = 2\mu H_b^{5/2}/\bar{D}$, where $\bar{D}$ is of the order of the depth of closure (Komar 1998; Falqués 2003). Our γ_x must be quite smaller than γ, as otherwise it would mask the large scale processes we are interested in. In case of the eastern storm and assuming $\bar{D} \simeq 8$ m the coastline diffusivity is $\gamma \simeq 0.2$ m^{2}s^{-1}, which is safely larger than 0.038. Therefore, our choice is sensible in this regard. Second, a too low diffusivity gives rise to the growth of small scale instabilities not related to the large scale physics which spoil down the simulation. Our choice $\epsilon_x = 0.02$ is at the lower bound to avoid this. Finally, a way to get a feeling for the correct range of the diffusivity is to consider that the time scale τ for the relaxation to the equilibrium profile if the profile is perturbed with a feature of lengthscale, L, is $\tau = L^2/\gamma_x$. Our choice would give $\tau = 3$ d in case $L = 100$ m which makes sense.

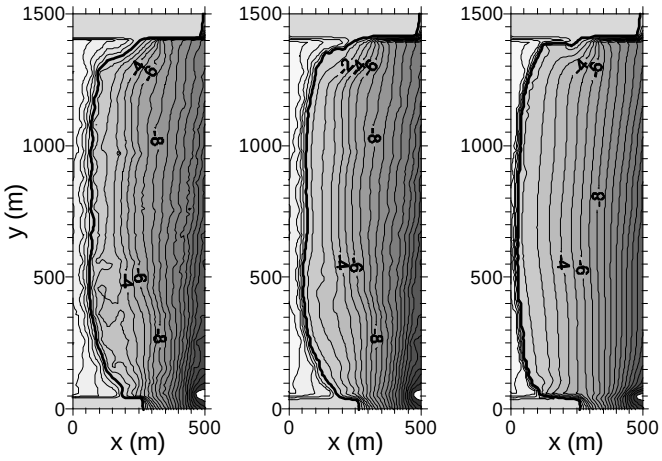

Figure 4. Model bathymetry. Left: initial one. Middle: before the eastern storm, October 15, 2003. Right: after the eastern storm, October 21, 2003.

4.2 Results

As seen in Fig. 4, the beach changes predicted by the model are rather minor before the E storm. A slight tendency to sand accumulation at the place where a megacusp very often develops ($y \simeq 500 - 600$ m) becomes apparent. With the start of the storm in October 15 a severe beach erosion occurs in the model resulting in a very pronounced regression of the shoreline (up to 50 m) at the end of the storm (October 20). As can be seen by comparing Figures 3 and 4, this was not observed in the final observed bathymetry on November 3. The reason for this is the following. The tendency of the model to predict beach erosion during a severe storm seems qualitatively correct according to common observations and is consistent with Ojeda and Guillén (2006) who describe some retreat in the shoreline of La Barceloneta by using video images. However, they also describe a subsequent recovery of the beach after the storm and this is not reproduced by the model in its present version. In contrast, the changes in the model bathymetry after the E storm are very small all the way to the end of the simulation, including the S-SW storm. The latter is not surprising as the wave energy arriving at la Barceloneta beach was quite small due to strong refraction and the storm

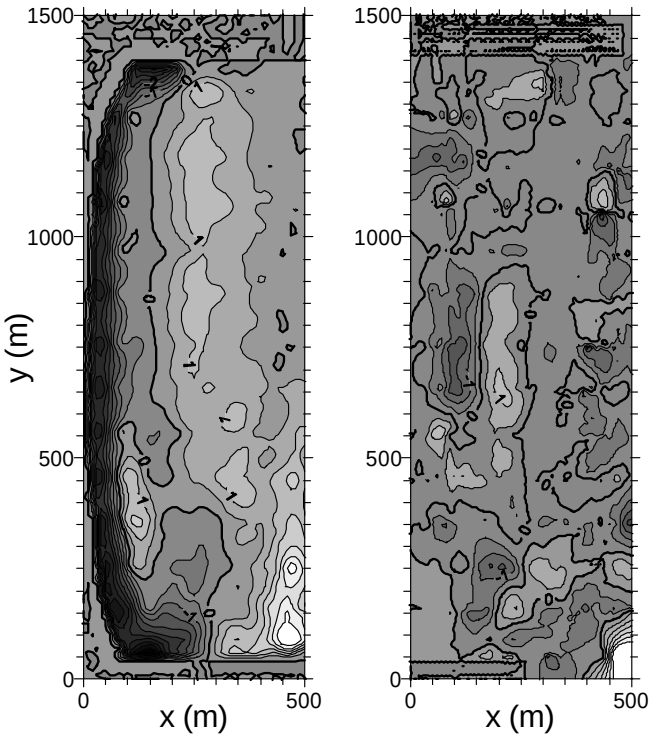

Figure 5. Differences in bed level between the final (November 3, 2003) and the initial (October 1, 2003) bathymetries. Dark colors mean erosion and ligh colors deposition. The zero contour line is inicated by a black thick line. Left: model. Right: observed.

duration was very short (about 1 day). This quasi 'inactivity' of the beach in the model during that period could correspond to the observed recovery process.

It becomes also apparent that the bathymetric lines in the model after the E storm become very smooth, much smoother than the observed ones. This results from the fact that the model replaces the complex surf zone processes as rip current circulation and rhythmic bars by the morphodynamic diffusivity and this is most dramatic during high energy events where this diffusivity is very large. This is however an expected limitation that is harmless for the aims of the model.

A more favorable comparison of model results with observed beach changes arises from the incremental bathymetries, i.e., substraction of initial bed levels to the final ones (Fig. 5). First, the generalized erosion close to the shoreline in most of the alongshore span of the beach is qualitatively reproduced by the model. At the southern tip of the beach this erosion area occurs farther offshore, in water depths $-4 < z_b < -2$ m, and this is also qualitatively predicted by the model. The erosion is however significantly overpredicted and this is specially dramatic at the shoreline. The counterpart of this erosion is sand deposition in a strip parallel to the coast at about $x \simeq 250$ m for $400 < y$ m that is apparent both in the modelled and in the measured bathymetry. The shapes of this sand accumulation area in both the model and reality are not identical. The main difference is that this 'incremental shoal' in the surveyed bathymetry weakens at its northern tip while in the model it is more alongshore uniform and overall more prominent. Also, in the southern part of the beach this accretion area is shifted offshore with respect to observations. The shore attachment of the deposition area corresponding with the megacusp in nature is not exactly reproduced in the model due to the exaggerated shoreline erosion. However, a very pronounced sand accumulation close to it (somewhat further south) is clearly apparent in the model indicating that the model tries to reproduce the megacusp. Finally, the model also catches the strong accretion area in deep water at the southern end of the beach which is represented in the 'observed' incremental bathymetry. This is because the initial bathymetry is very deep at this area (strongly off-equilibrium) and the model tries to replenish this region. In the final observed bathymetry, this region is indeed less deep so that model and observations tend to coincide. However, as it has already been noted, the high water depths at this area could be (partially) an artifact of the gridding so as both model and 'observed' bathymetry might overestimate this deposition tendency.

5 DISCUSSION AND CONCLUSIONS

An extension of one-line coastline models to include cross-shore beach profile dynamics has been presented. The extension is conceptually in the same direction as the N-line models but the rationale of the new model is quite different from them. Essentially, rather than moving the contour lines as those models do, the present model updates the bed levels in a rectangular grid as the common 2DH models do. Thus, it can be considered a quasi- 2DH model and it might be quite easy in the future to build a unified model capable of running alternatively as 2DH or as quasi-2DH. The model has been tested against morphological changes in an embayed beach. This is a rather unfavorable case study for such sort of models because they are mainly meant to predict gross changes in shoreline rather than detailed bathymetric changes. This is specially so as no significant shoreline changes were observed on that beach during the simulation period. Nevertheless, we wished to do this first test of the model in the worst performance conditions.

A period of 35 days which include two storms, one from the E and another from the S-SW was simulated. To keep the model running for such a long period and producing reasonable bathymetry and waves was not trivial at the beginning but was finally accomplished (for instance, the Bailard formulation for cross-shore transport was rather unstable from a numerical point

of view). However, the comparison of the final modelled bathymetry with the final observed one shows significant differences in some respects. In particular there is a very strong shoreline retreat which was not observed in the final bathymetry. This is very likely due to the failure of the model to describe post-storm recovery rather than an incorrect prediction of beach erosion during a severe storm. Furthermore, the contour lines in the model are smoother than in nature although it is not surprising since the model filters out surf zone morphodynamic medium scale features. In contrast, an analysis of the incremental bathymetries (differences in bed level between the initial bathymetry and the final one) reveals an encouraging qualitative similitude between the main tendencies in the bathymetric evolution of both model and observations. For instance, erosion close to the shore and deposition further offshore is well reproduced by the model. Besides, nearly in the alongshore location where a megacusp develops in the observed shoreline, the model predicts a significant sand accumulation. This test is still very preliminary but it suggests that the model has potential skill for beach change prediction. Work is currently under way to investigate the sensitivity of the model results to the parameters describing cross-shore transport and shoreline evolution. In particular, the reasons for the too strong shoreline retreat/inability of beach recovery are being investigated. Given the relatively good qualitative results of the model in predicting deposition/erosion out of the shoreline, once the shoreline description will improve the model will likely perform much better. This will be hopefully discussed at the Conference.

6 ACKNOWLEDGEMENTS

This research is part of the PUDEM project, funded by the Spanish Government under contracts REN2003-06637-C02-01/MAR and REN2003-06637-C02-02/MAR. Partial funding from the CTM2006-08875/MAR project is also gratefully acknowledged. The work of E. Ojeda and F. Ribas are supported by the Spanish Government through the programs FPU and Juan de la Cierva, correspondingly.

REFERENCES

Ashton, A. and A. B. Murray (2006). High-angle wave instability and emergent shoreline shapes: 1. modeling of sand waves, flying spits, and capes. *J.Geophys.Res. 111*, F04011,doi:10.1029/2005JF000422.

Ashton, A., A. B. Murray, and O. Arnault (2001). Formation of coastline features by large-scale instabilities induced by high-angle waves. *Nature 414*, 296–300.

Bailard, J. A. (1981). An energetics total load sediment transport model for a plane sloping beach. *J. Geophys. Res. 86*(C11), 10938–10954.

Calvete, D., N. Dodd, A. Falqués, and S. M. van Leeuwen (2005). Morphological development of rip channel systems: Normal and near normal wave incidence. *J. Geophys. Res. 110*(C10006). doi:10.1029/2004JC002803.

Dabees, M. and J. W. Kamphuis (2000). Nline: effi cient modeling of 3-d beach changes. In *Coastal Eng. 2000*, vol. 3, pp. 2700–2713. Am. Soc. of Civ. Eng.

Falqués, A. (2003). On the diffusivity in coastline dynamics. *Geophys. Res. Lett. 30*(21), 2119. doi:10.1029/2003GL017760.

Falqués, A. (2006). Wave driven alongshore sediment transport and stability of the Dutch coastline. *Coastal Eng. 53*, 243–254.

Falqués, A. and D. Calvete. (2003). Propagation of coastline sand waves. In A. Sánchez-Arcilla and A. Bateman (Eds.), *Proc. 3^{rd} IAHR symposium on River, Coastal and Estuarine Morphodynamics*, vol. 2, Barcelona, Spain, pp. 903–912.

Falqués, A. and D. Calvete (2005). Large scale dynamics of sandy coastlines. Diffusivity and instability. *J. Geophys. Res. 110*(C03007). doi:10.1029/2004JC002587.

Garnier, R., D. Calvete, A. Falqués, and M. Caballeria (2006). Generation and nonlinear evolution of shore-oblique/transverse sand bars. *J. Fluid Mech. 567*, 327–360.

Horikawa, K. (1988). *Nearshore Dynamics and Coastal Processes*. Tokio, Japan: University of Tokio Press.

Inman, D. L. (1987). Accretion and erosion waves on beaches. *Shore and Beach 55*(3/4), 61–66.

Kirby, J. T. and R. A. Dalrymple (1994). Combined refraction/diffraction model REF/DIF1, Version 2.5. Res. Report CACR-94-22, Center for Applied Coastal Research, Univ. of Delaware.

Komar, P. D. (1998). *Beach Processes and Sedimentation* (Second ed.). Prentice Hall.

Larson, M., H. Hanson, and N. C. Kraus (1987). Analytical solutions of the one-line model of shoreline change. Technical report, US Army Corps of Engineers.

Larson, M. and N. C. Kraus (1991). Mathematical modeling of the fate of beach fi ll. *Coastal Eng. 16*, 83–114.

Ojeda, E. and J. Guillén (2006). Monitoring beach nourishment based on detailed observations with video measurements. *J. Coastal Res. SI 48*, 100–106.

Pelnard-Considère, R. (1956). Essai de theorie de l'evolution des formes de rivage en plages de sable et de galets. In *4th Journees de l'Hydraulique, Les Energies de la Mer, Paris*, Volume III(1), pp. 289–298. Société Hydrotechnique de France.

Ruessink, B. G. and M. C. J. L. Jeuken (2002). Dunefoot dynamics along the dutch coast. *Earth Surface Processes and Landforms 27*, 1043–1056.

Short, A. D. (1999). *Handbook of Beach and Shoreface Morphodynamics*. Chichester: Wiley.

Steetzel, H. J., J. H. de Vroeg, L. C. van Rijn, and J. M. Stam (1998). Morphological modelling using a modifi ed multi-layer approach. In *Coastal Eng. 1998*, pp. 2368–2381. Am. Soc. of Civ. Eng.

Thevenot, M. M. and N. C. Kraus (1995). Longshore sandwaves at Southampton Beach, New York: observations and numerical simulation of their movement. *Mar. Geology 126*, 249–269.